

Physics-based Creep Simulations of Thick Section Welds in High Temperature and Pressure Applications

Thomas M. Lillo, PI

Wen Jiang, Co-Investigator

Idaho National Laboratory

P.O. Box 1625

Idaho Falls, ID 83415

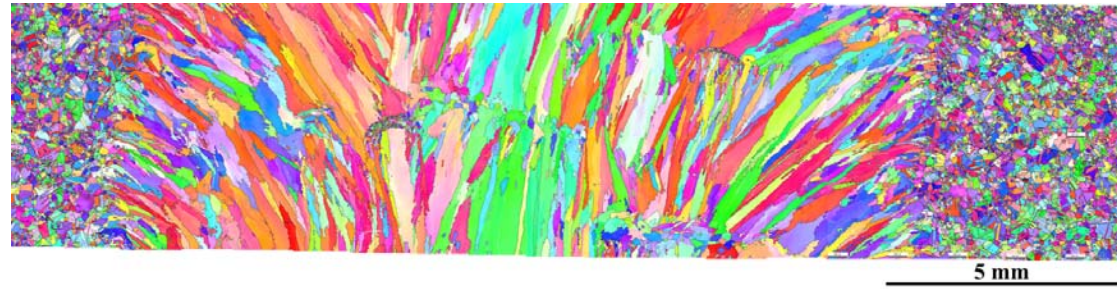
Thomas.Lillo@INL.gov

**2017 NETL Crosscutting Research & Analysis Program
Portfolio Review, March 20-23, 2017, Pittsburgh, PA**

Date: March 22, 2017

DOE Award Number: FEAA90

Period of Performance: 07/2015-07/2018



Project Goals and Objectives

Goal: Develop modeling and simulation capabilities to describe/predict the creep behavior of thick section welds in Alloy 740H

- Computational modeling development of physical processes involved in the creep of welds in Alloy 740H across length scales:
 - Diffusion
 - Dislocation motion and deformation
 - Microstructural evolution
 - Uniaxial creep specimen behavior
- Develop/modify individual computational “modules” to describe each physical process:
 - Dislocation glide/climb
 - Dislocation/ γ' interaction
 - γ' shearing
 - Dislocation climb over γ' particles
 - Dislocation looping of γ'
 - Incorporate experimental microstructures and their evolution
 - Diffusional creep
 - Grain boundary sliding

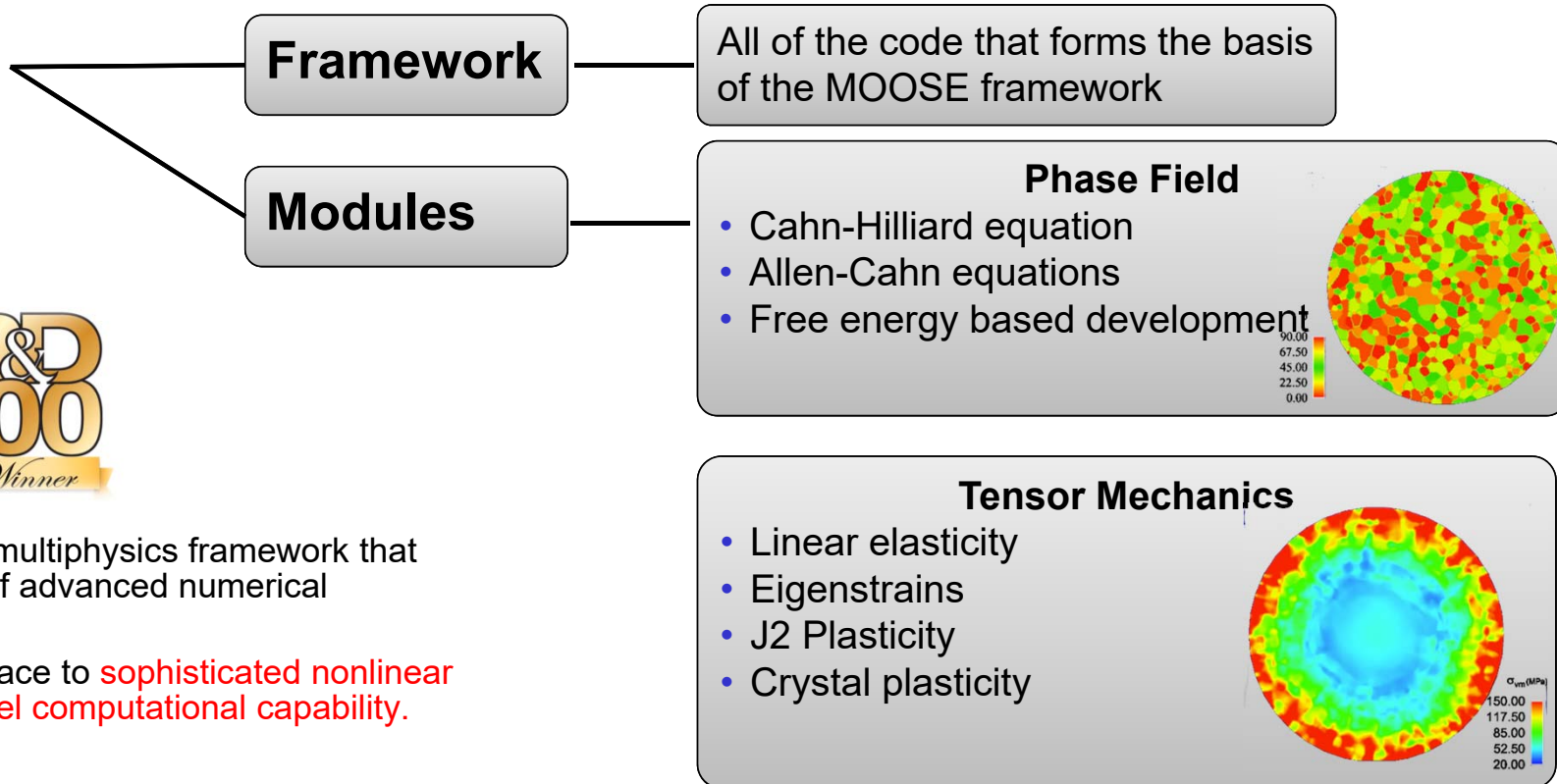
Project Goals and Objectives – cont.

- Experimental Validation
 - Creep tests – different stresses and temperatures
 - γ' aging
 - Weld
 - HAZ
 - Base metal (if necessary)
 - Threshold stress as a function of γ' evolution – dislocation/ γ' interaction as a function of γ' radius
 - Microstructural characterization for the generation of synthetic microstructures
 - Weld
 - HAZ
 - Base metal

Presentation Outline

- Modeling and simulation approach
 - Overview of the MOOSE architecture
 - Power law creep – incorporation of dislocation climb
 - Dislocation interaction with γ' particles
 - Particle shearing
 - Dislocation climb bypass
 - Orowan looping
- Experimental Studies supporting modeling
 - Creep tests of weld
 - Microstructural characterization using EBSD
 - γ' Aging
 - Threshold stress determination

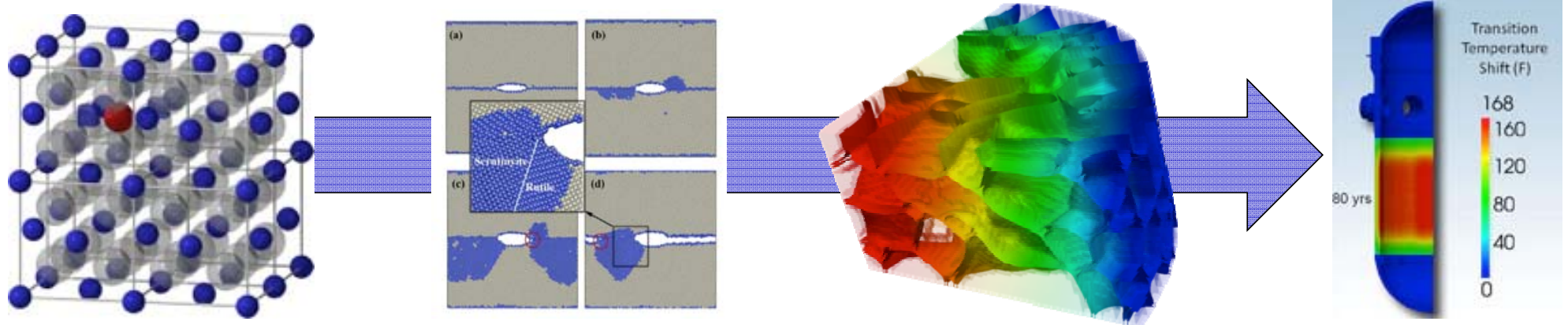
Modeling and Simulation Approach – MOOSE Architecture



- MOOSE is a finite element, multiphysics framework that **simplifies the development** of advanced numerical applications.
- It provides a high-level interface to **sophisticated nonlinear solvers and massively parallel computational capability**.
- Open Source, available at <http://mooseframework.org>

Physical based Multi-scale Material Model Development

- Atomistic simulations identify critical mechanisms and determine parameters required for mesoscale model development.
- Mesoscale modeling and simulation is used to inform the development of analytical theory for engineering scale.



nanometers

First Principles

- Identify critical bulk mechanisms
- Determine bulk properties

100's of nanometers

Molecular Dynamics

- Identify interfacial mechanisms
- Determine interfacial properties

microns

Mesoscale

- Predict microstructure evolution
- Determine impact on properties

millimeters and up

Engineering scale

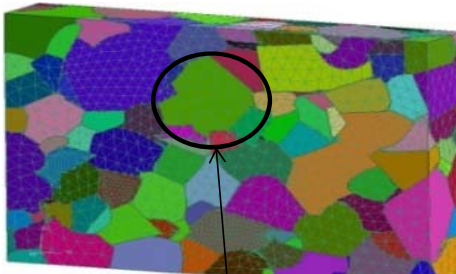
- Use analytical theory
- Predict material performance

Modeling Approach

- Polycrystalline length scale – region consisting of base metal, HAZ and fusion region
- FIB, EBSD, SEM – Grain size, orientation, misorientation distribution
- Reconstructed or synthetic microstructure satisfying the statistics

Diffusional creep:

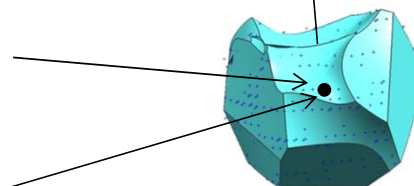
Vacancy generation/annihilation model



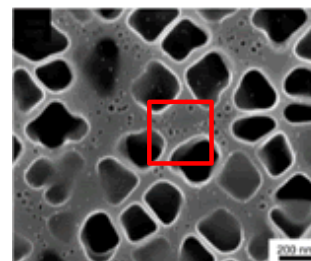
Representative Volume of polycrystalline microstructure

Dislocation creep:

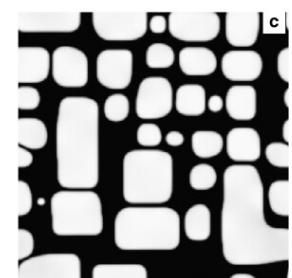
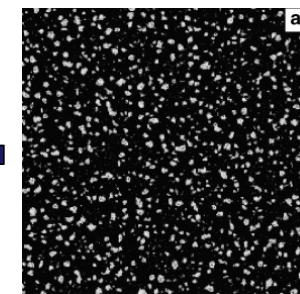
Dislocation density based model
considering APB shearing,
Orowan loop and climb



Effect of γ' shape, size, volume fraction
on APB shear - Homogenized model
from micromechanics simulation

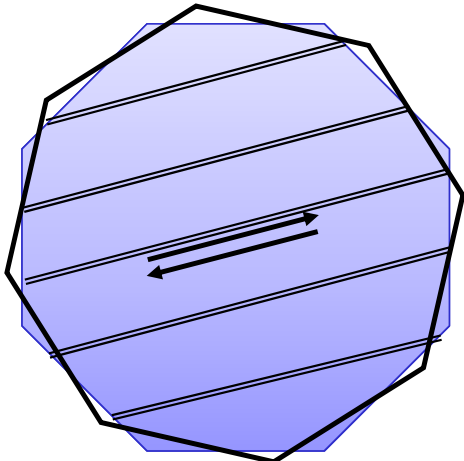


Evolution of γ' precipitate



Crystal plasticity Model (dislocation density based)

- Crystal plasticity mechanistically represents plastic deformation by representing dislocation slip along slip planes
- Slip contributions are summed across all slip planes



Dislocation motion
defined by a flow rule

$$\dot{\gamma}^s = \tilde{\dot{\gamma}}^s(\tau^s, \tau_0^s)$$

Dislocation generation and pile-up
accounted for by increasing slip resistance
with a hardening law

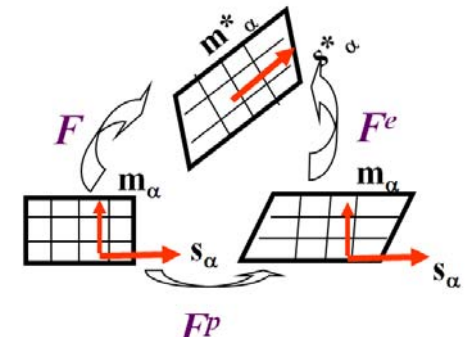
$$\mathbf{F} = \mathbf{F}^V \mathbf{F}^e \mathbf{F}^p \quad \text{Volumetric can account for residual strains}$$

Plastic velocity gradient in the intermediate configuration

$$\dot{\mathbf{F}}^p \mathbf{F}^{p-1} = \sum_{\alpha} \dot{\gamma}_{\text{glide}}^{\alpha} \mathbf{S}_0^{\alpha} + \sum_{\alpha} \dot{\gamma}_{\text{climb}}^{\alpha} \mathbf{N}_0^{\alpha}$$

$$\mathbf{S}_0^{\alpha} = \mathbf{s}^{\alpha} \otimes \mathbf{m}^{\alpha} \quad \mathbf{N}_0^{\alpha} = \mathbf{s}^{\alpha} \otimes \mathbf{s}^{\alpha}$$

\mathbf{s}^{α} - Slip direction \mathbf{m}^{α} - normal in reference configuration



Glide model

Glide rate in matrix $\dot{\gamma}_{glide}^{\alpha} = \rho_M^{\alpha} b v_{glide}^{\alpha}$

(ρ_M – Potentially mobile dislocation density)

Glide velocity:

$$v_{glide}^{\alpha} = \begin{cases} l v \exp\left(-\frac{\Delta F_{glide}}{KT} \left(1 - \left(\frac{|\tau^{\alpha}| - g_{athermal}^{\alpha}}{g_{thermal}^{\alpha}}\right)^p\right)^q\right) \operatorname{sgn}(\tau^{\alpha}); & \text{for } |\tau^{\alpha}| > g_{athermal}^{\alpha} \\ 0 & \text{otherwise} \end{cases}$$

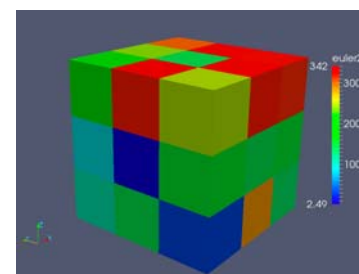
Resolved shear stress $\tau^{\alpha} = \mathbf{T}^* : \mathbf{S}_0^{\alpha}$

Athermal resistance: $g_{athermal}^{\alpha} = \sqrt{\left(\tau_{disloc-disloc}^{\alpha}\right)^2}$

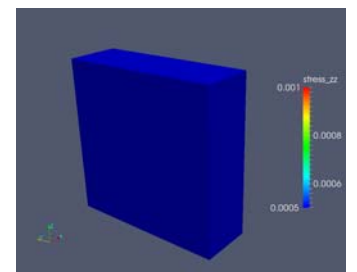
$$\tau_{disloc-disloc}^{\alpha} = q_{\rho} G b \sqrt{\sum A^{\alpha\xi} \rho^{\xi}}$$

Numerical example

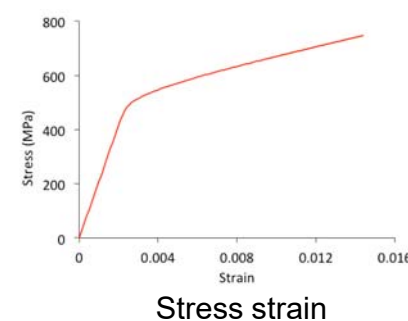
- $75 \times 75 \times 75 \mu\text{m}$ unit cube
- 27 grains randomly oriented
- 3375 elements
- Uniaxial tension with symmetric boundary condition
- Non-calibrated parameters



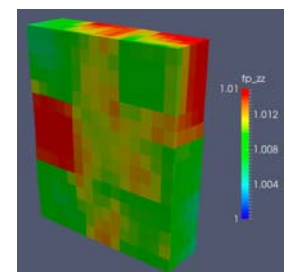
Euler Angle (θ)



Stress Evolution



Stress strain



Anisotropic plastic deformation

Climb model

Edge component of dislocation will climb

Climb stress

$$\tau^\alpha = \mathbf{T}^* : \mathbf{N}_0^\alpha = \frac{RT}{V_m} \ln\left(\frac{c^{*\alpha}}{c}\right)$$

c^* - vacancy concentration at dislocation core

c - vacancy concentration in surrounding matrix

Equilibrium concentration at dislocation core

$$c^{*\alpha} = c_0 \exp\left(\frac{k\tau^\alpha V_m}{RT}\right)$$

k : factor that depends on precipitate size, shape, etc

Climb velocity

$$v_c^\alpha = -\frac{2\pi D}{b \log(r_p / r_c)} (c^{*\alpha} - c_0)$$

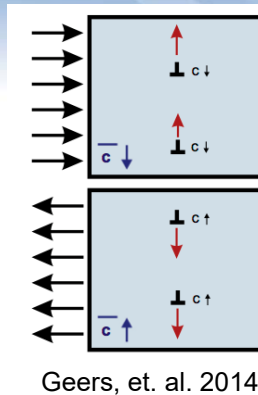
Effect of dislocation density on effective radius

$$r_p = \frac{1}{2\sqrt{\sum(\rho_M^\alpha + \rho_I^\alpha)}}$$

Core radius $r_c = 4b$ r_p = radius where $c^* \sim c$

Climb rate:

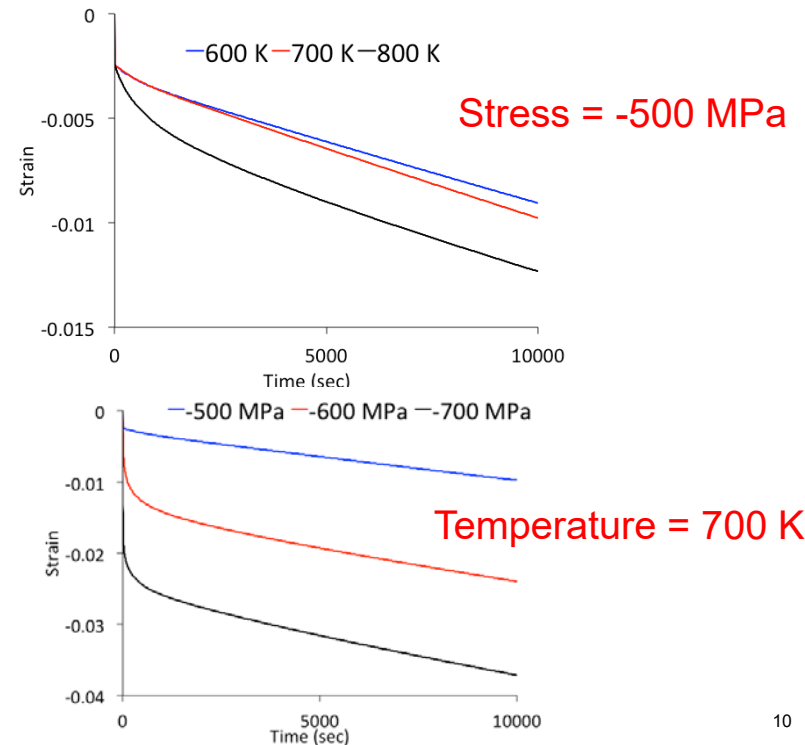
$$\dot{\gamma}_c^\alpha = (\rho_M^\alpha + \rho_I^\alpha) b v_c^\alpha$$



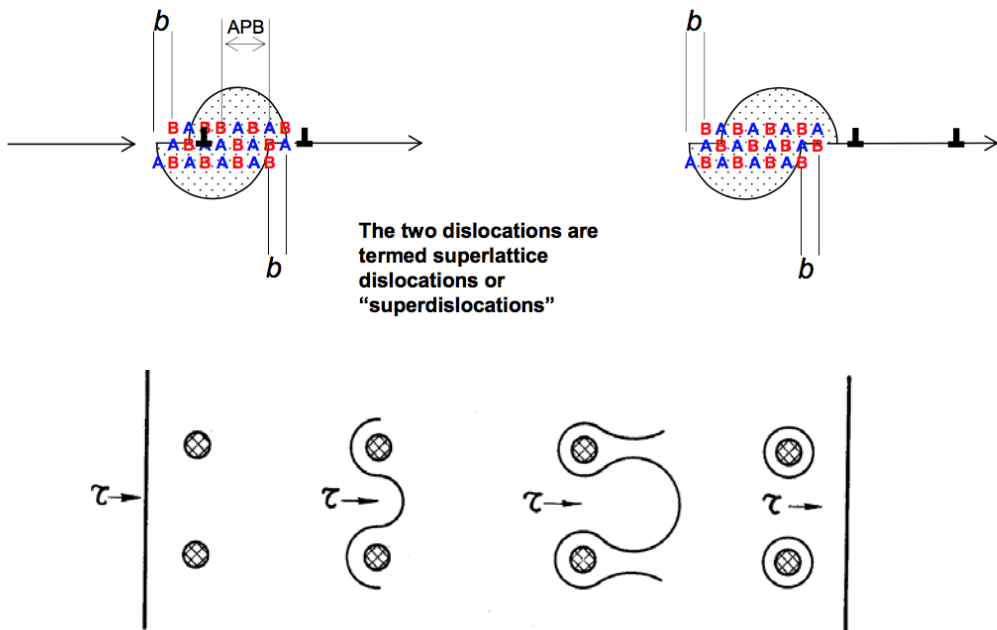
Geers, et. al. 2014

Numerical example

- $1 \times 1 \times 1 \mu\text{m}$ unit cube
- Single crystal with one element
- Creep compression with symmetric boundary condition



APB (Shearable) and Looping (Nonshearable)



- APB formation modifies the atomic structure of the ordered γ'
- Orowan looping occurs when looping is easier than cutting.

Slip resistance:

$$\tau_{\text{disloc-ppt}} = \frac{1}{2b^2 r} \sqrt{\frac{3f\bar{F}}{\pi G\beta}}$$

Shearable: $r < r_c$

$$\bar{F} = 2\beta G b^2 \left(\frac{r}{r_c}\right)$$

Non-shearable: $r > r_c$

$$\bar{F} = 2\beta G b^2$$

r_c :critical radius of precipitate

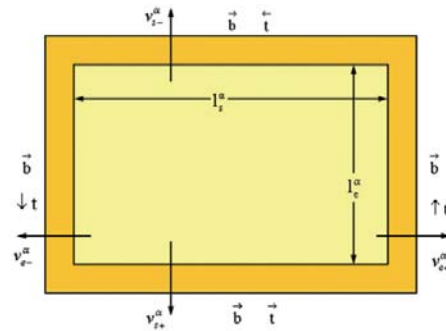
Athermal resistance:

$$g_{\text{athermal}}^\alpha = \sqrt{\left(\tau_{\text{disloc-disloc}}^\alpha\right)^2 + \boxed{\left(\tau_{\text{disloc-ppt}}^\alpha\right)^2}}$$

Dislocation density evolution

Dislocation density evolution

$$\dot{\rho}^\alpha = \dot{\rho}_M^\alpha + \dot{\rho}_I^\alpha$$



Evolution of mobile dislocation density

$$\dot{\rho}_M^\alpha = \frac{k_{mul}}{b} \sqrt{\sum_\beta \rho_M^\beta} |\dot{\gamma}_{glide}^\alpha| - \frac{2R_c}{b} \rho_M^\alpha |\dot{\gamma}_{glide}^\alpha| - \frac{1}{b\lambda^\alpha} |\dot{\gamma}_{glide}^\alpha| + C_1 |\dot{\gamma}_{climb}^\alpha| + C_2 |\dot{\gamma}_{ppt}^\alpha|$$

Dislocation multiplication from Frank-Read source and loop expansion

Annihilation of dislocations of opposite signs

Dislocation trapping

Mobilization of Dislocations

Evolution of immobile dislocation density

$$\dot{\rho}_I^\alpha = \frac{1}{b\lambda^\alpha} |\dot{\gamma}_{glide}^\alpha| - C_3 |\dot{\gamma}_{climb}^\alpha| - C_4 |\dot{\gamma}_{ppt}^\alpha|$$

Dislocation trapping

Mobilization of Dislocations

Mean trapping distance

$$\frac{1}{\lambda^\alpha} = \beta_\rho \sqrt{\rho^\alpha} + \beta_{ppt} \sqrt{Nd}$$

Modular model development

Integration at every material point

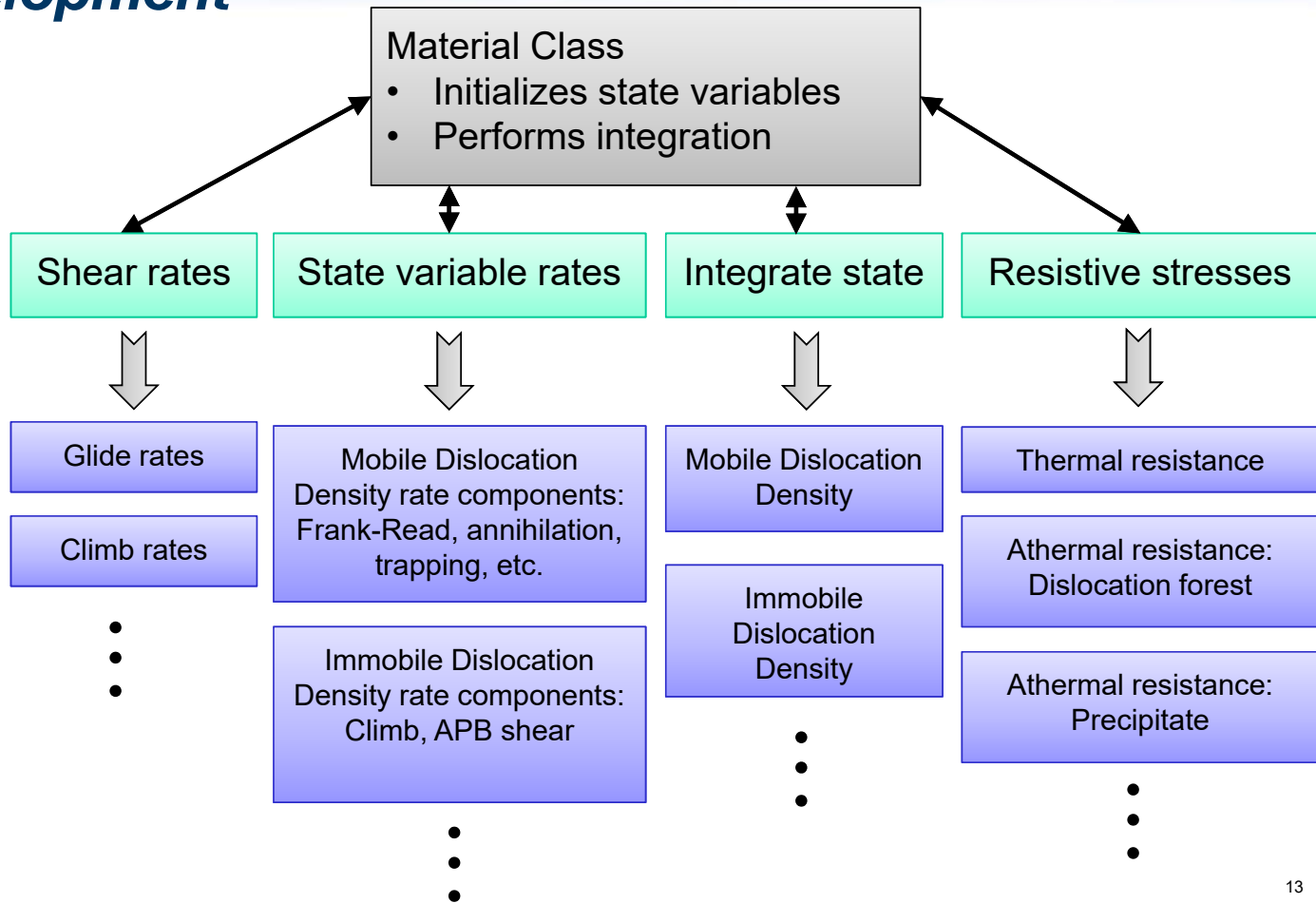
- Newton-Raphson for stress

$$T_{n+1}^{i+1} - \tilde{T}_{n+1}^{i+1}(F_{n+1}^{p,i+1}, y_{n+1}^j) = 0$$

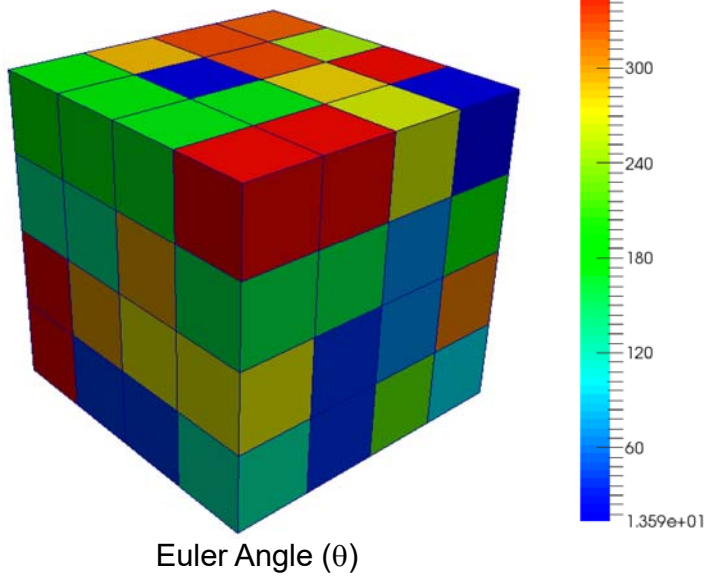
- Fixed-point iteration for state

$$y_{n+1}^{j+1} = f(T_{n+1}^{i+1}, F_{n+1}^{p,i+1}, y_{n+1}^j)$$

till $|y_{n+1}^{j+1} - y_{n+1}^j| < \eta$

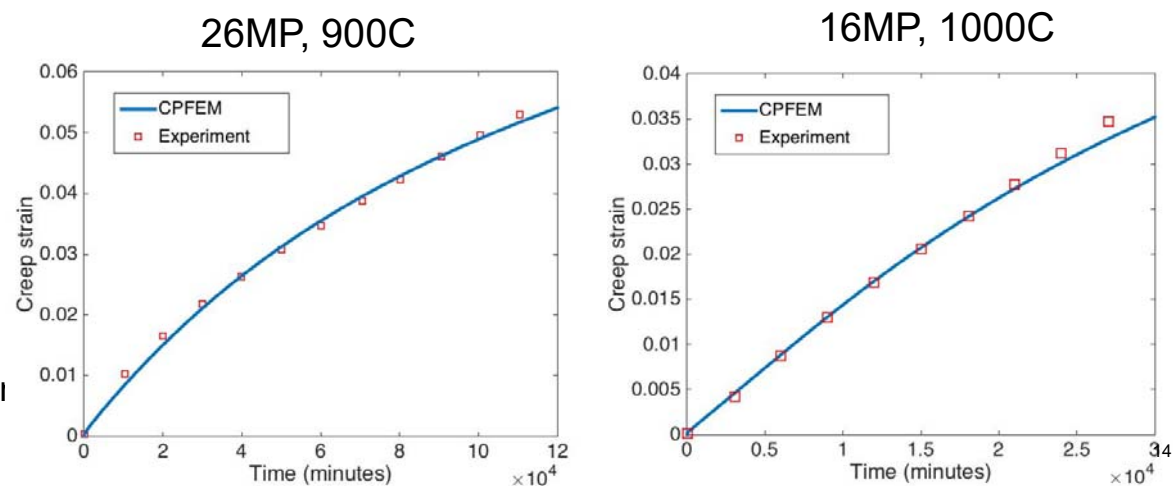


Initial calibration of Alloy 617



- $500 \times 500 \times 500 \mu\text{m}$ unit cube
- 64 grains randomly oriented
- Uniaxial tension with symmetric boundary conditions

C11	C12	C44	G
170.64Gpa	108.39Gpa	77.82Gpa	77.82Gpa
p	q	Activation Entropy(J)	Thermal Resistance
0.78	1.15	5.148×10^{-19}	0.5
Barrier factor	Self harden Factor	Latent harden factor	Multiplication factor
0.045	0.052	0.052	0.01



Experimental Studies – Creep Testing

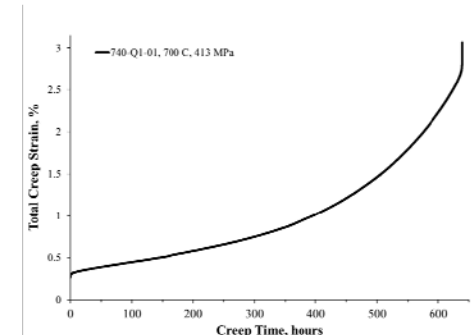
- Creep tests will be carried out at or below the aging temperature
 - Short/intermediate term creep tests – support modeling and validation of modules
 - All-weld metal gage section
 - Longitudinal
 - Transverse – compression creep sample
 - Transverse gage section
 - Creep stresses to yield test duration between 200-2000 hrs (Larson-Miller plot, Special Metals datasheet for Alloy 740H implies 140 - 400 MPa for welds)
 - Long term creep test – validate simulation
 - 141 MPa, 750°C, ~9700 hrs (expected)
 - 83 MPa, 800°C, ~9700 hrs (expected)



Specimen ID	Test temperature, °C	Test type	Initial Stress, MPa	Orientation	Expected rupture life, hrs	Start date	Finish date	Rupture life, Hrs
740-Q1-01	700	Rupt	413	CW*	200	8/24/2016	9/21/2016	639
740-Q1-08	700	Rupt	413	CW	500	11/28/2016	12/27/2016	670.8
740-Q1-06	700	Rupt	395	CW	1000	01/09/2017		
	700	Rupt	344	CW	1000			
740-Q1-03	750	Rupt	350	CW	200	9/29/2016	10/07/2016	184
740-Q1-05	750	Rupt	305	CW	500	10/18/2016	11/06/2016	450
	750	Rupt	213	CW	1000			
740-Q1-04	800	Rupt	240	CW	200	10/10/2016	10/15/2016	123.6
740-Q1-02	800	Rupt	200	CW	500	11/08/2016	11/22/2016	326.8
	800	Rupt	138	CW	1000			
	700	Rupt	400	AWM**	500			
	750	Rupt	248	AWM	500			
	800	Rupt	144	AWM	500			

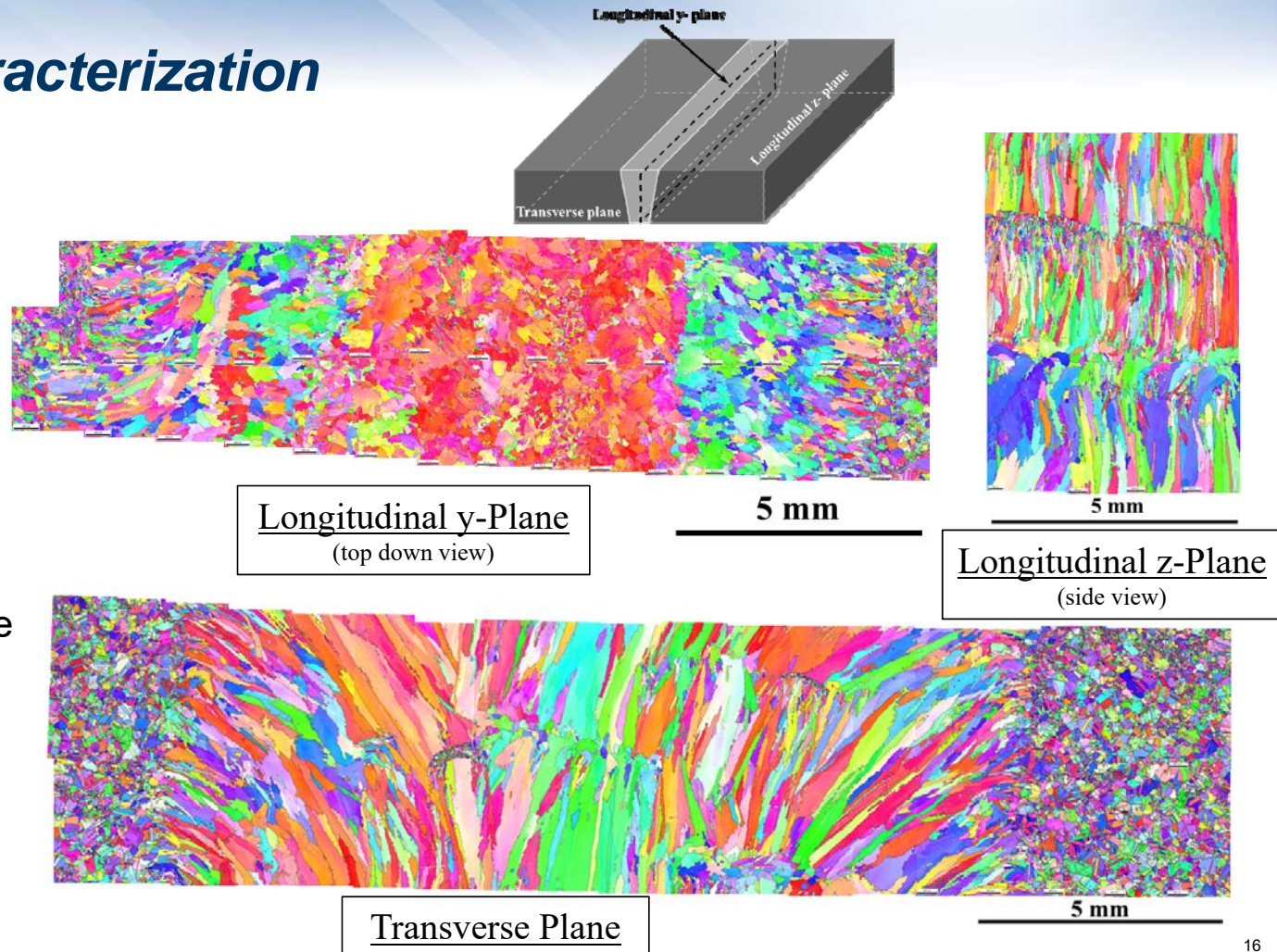
* CW = Cross weld

** AWM = All Weld Metal



Microstructural Characterization

- Optical metallography and EBSD on three orthogonal surfaces
- Includes base metal, HAZ and weld metal
- Grain Morphology
- Orientation and misorientation statistics
- Supports generation of synthetic microstructures
- Solidification segregation in the weld metal
- γ' size & volume fraction -TEM
 - Base metal
 - HAZ
 - Weld metal

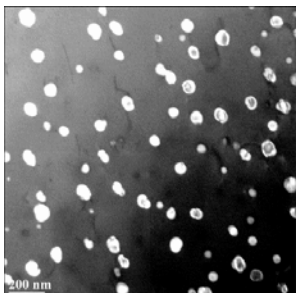


γ' Aging

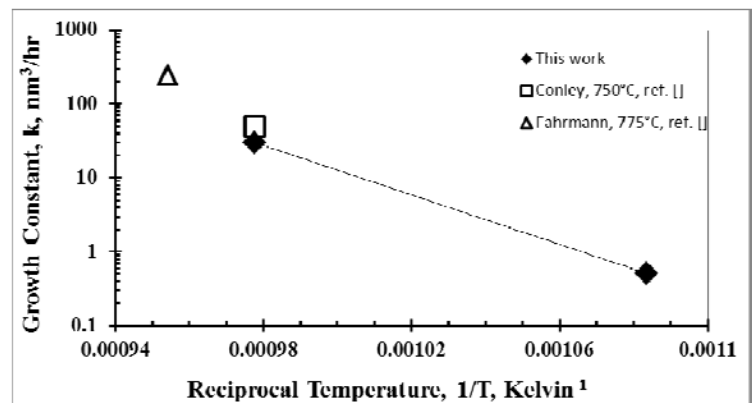
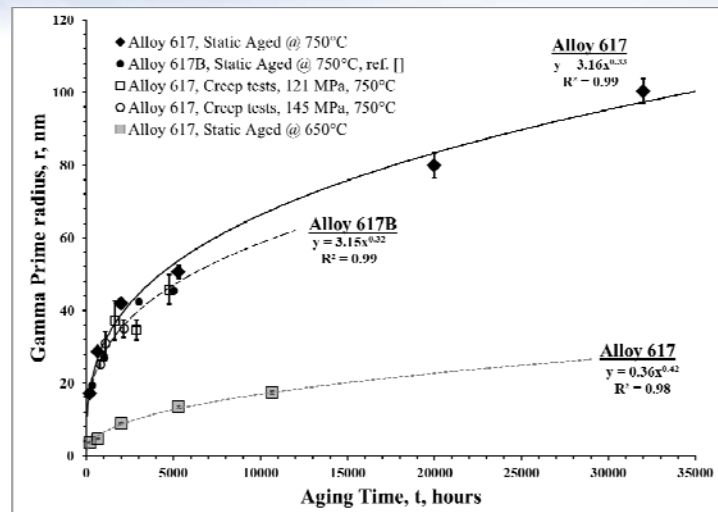
- γ' growth and compositional homogenization
- Base metal and weld metal (compositional effects?)
- Determine growth constant for γ' for modeling effort:

$$r^3 - r_0^3 = kt$$

- Temperatures: 700, 750, 800°C
- Times: 50, 100, 200, 400, 1000, 3000, 6000 and 10,000 hrs
- TEM with image analysis

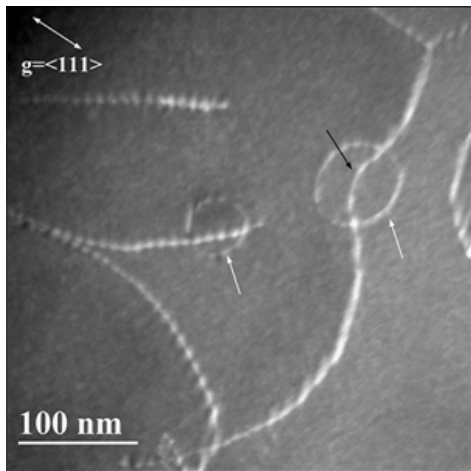


Alloy 617, 750°C,
145 MPa, $e=5\%$,
 ~ 1083 hrs

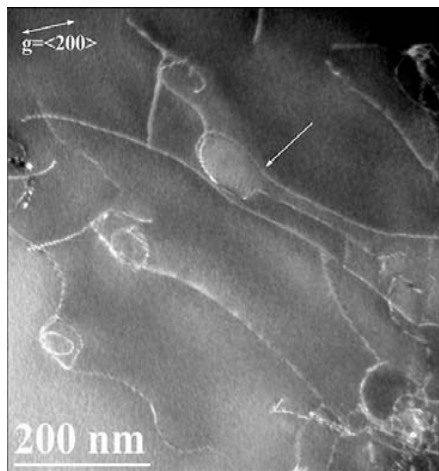


Threshold Stress Determination

- Threshold stress is determined by primary dislocation bypass mechanism of the γ' particles
- Threshold stress determined by stress drop creep tests

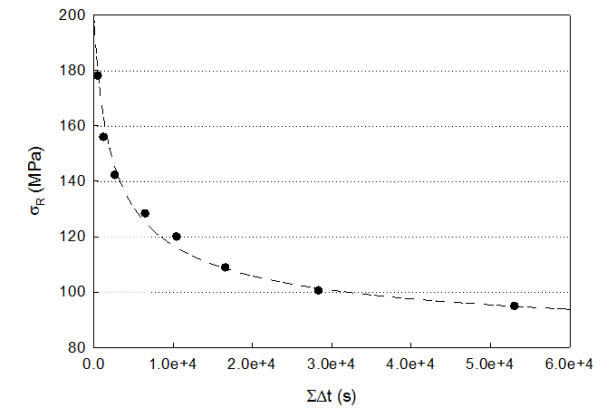
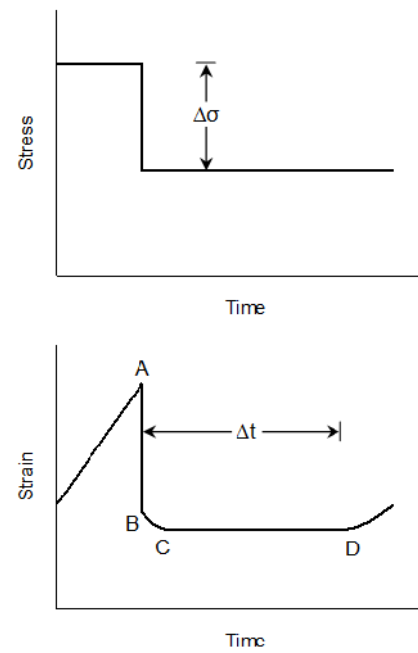


γ' particle bypass by
dislocation climb



γ' particle bypass by
dislocation looping

Bypass mechanisms in Alloy 617



$$\Sigma\Delta t = \frac{\mu^2 b^2}{K} [(\sigma_R - \sigma_0)^{-2} - (\sigma_t - \sigma_0)^{-2}]$$

Questions

Contact Information

- Thomas Lillo:
 - Thomas.Lillo@inl.gov
 - (208)526-9746
- Wen Jiang:
 - Wen.Jiang@inl.gov
 - (208)526-1586